Optimal Design of Three-Dimensional Structures with Hysteretic Braces

G. Apostolakis
Sprung-brett RDI Inc., Baird Research Park
University at Buffalo, the State University of New York, USA

G.F. Dargush
University at Buffalo, the State University of New York, USA

15 WCEE
LISBOA 2012

SUMMARY:
Current seismic codes incorporate well-established simplified approaches to protect and mitigate the response of structures under extreme events using hysteretic passive devices. Nevertheless, a systematic and well-establish methodology for the topological distribution and properties of these devices in three-dimensional structures does not exist. In this paper, we develop a computational framework to evolve optimal brace configurations for complicated three-dimensional regular and irregular structures within a given seismic environment consisting of four synthetic ground motions (5% exceedance in 50 years). Non-linear transient dynamic analyses, based upon a Mixed Lagrangian Formulation, are used to evaluate the structures, while the optimization is accomplished with a compact Cellular Automata-based Genetic Algorithm. As a result of the evolutionary process, the optimal placement, strength and size of the dampers are obtained for regular and irregular eight-story steel frame buildings. Interesting brace patterns evolve from the discrete optimization process.

Keywords: passive energy dissipation, optimal design, mega-braces, irregular structure, topology optimization

1. INTRODUCTION

Modern state-of-the-art seismic codes provide well-established approaches for structural design in order to prevent collapse and loss of life in extreme events. Many of these approaches involve innovative seismic protection systems that have been developed in the past decades and have been extensively validated both numerically and experimentally. These technologies can be mainly categorized into damping and isolation systems. In the present paper we are interested in studying damping systems and more specifically yielding metallic dampers (*e.g.*, Buckling Restrained Braces). Yielding metallic passive devices have been used, in the design of new structures as well as in retrofitting existing structures, in order for the structures to withstand the expected seismic motion by dissipating energy through yielding of steel (*e.g.*, Soong and Dargush, 1997). Therefore, the amount of energy dissipated by these devices is dependent on the yield load. Moreover, it is a common practice that the distribution of these devices throughout the height of structures is based on the elastic mode shapes (FEMA-273, 1997; FEMA-274, 1997). This would be sufficient if the structure remained elastic, but since the structures (even with energy dissipative devices) are not expected to remain elastic during design and extreme earthquake events, this approach will eventually lead to a non-optimal utilization of the passive devices. Moreover, the distribution of the ductility demand throughout the structure is not expected to be uniform. Therefore, the topological distribution of the hysteretic dampers is critical in the overall performance of the structure under seismic loadings.

The passive damper topological distribution problem has been addressed previously by a number of researchers, including Zhang and Soong (1992), Gluck *et al.* (1996), Takewaki (1997), Singh and Moreschi (2001, 2002), Moreschi and Singh (2003), Lavan and Levy (2005, 2006), Levy and Lavan (2006), Dargush and Sant (2005) and Lavan and Dargush (2009), In recent work by the present authors, a systematic methodology was developed for optimizing the topological distribution and size of hysteretic devices in order to achieve a desired response performance for planar structures

(Apostolakis and Dargush, 2010). In that paper, a computational framework is proposed for the optimal distribution and design of yielding metallic buckling restrained braces (BRB) and/or friction dampers within steel moment-resisting frames (MRF) for a given seismic environment. Performance objectives relate to satisfying both drift and acceleration criteria. Non-linear dynamic analysis is conducted using DRAIN2D (Prakash, 1993) to assess performance and a simple Genetic Algorithm (GA; Holland, 1992) is used to solve the resulting discrete optimization problem. Specific examples involving two three-story, four-bay steel MRFs and a six-story, three-bay steel MRF retrofitted with yielding and/or friction braces are considered. Interestingly, in all cases, the brace configurations evolve to form arch-like elements within the overall structure.

What types of brace configurations would evolve in more complicated three-dimensional regular and irregular structures? To answer this question, in the present work, we extend the above approach to spatial frames. The non-linear transient dynamic analysis now is performed using the Mixed Lagrangian Formalism (MLF; Sivaselvan and Reinhorn, 2006; Sivaselvan *et al*., 2009) and the optimization is accomplished with a compact Cellular Automata-based Genetic Algorithm (CA-GA; Barmpoutis and Dargush, 2007). The seismic environment consists of four synthetic ground motions representative of the west coast of the United States with 5% probability of exceedance in 50 years. As a result of the evolutionary process, the optimal placement, strength and size of the dampers are obtained for regular three-, eight- and fifteen-story steel frame buildings, along with an irregular eight-story structure. Again, interesting brace patterns evolve from the discrete optimization process. In this paper, the focus is on the eight-story structures.

2. COMPUTATIONAL FRAMEWORK

A computational framework is proposed for the optimal design of three-dimensional structures with hysteretic braces. The objective is to find a topological distribution and the size and yielding level of the devices throughout the height of the structure. For realistic applications one has to assume all the combinations of brace patterns that can be retrofitted to every bay of the structure and a range of parameters for the size and yield level of the braces. As a result, the number of the possible design configurations becomes very large and prohibitive to exhaustive search. Therefore, for the optimal design of realistic three-dimensional structures desirable features of the computational framework are a numerical method that can provide accurate and efficient non-linear transient dynamic analysis results and an optimization approach that can provide a systematic and robust methodology for exploiting good solution from a very large search space. For the former, we use the Mixed Lagrangian Formalism (MLF) approach and for the latter we incorporate a compact Cellular Automata-based Genetic Algorithm. The performance of the individual designs is evaluated using a fitness function strategy.

2.1. Mixed Lagrangian Formalism

In this paper non-linear transient dynamic analysis, for the evaluation of the structures, is performed using a Mixed Lagrangian Formalism (MLF) approach (Sivaselvan and Reinhorn, 2006). The weak formulation starts with the proper selection of state variables and the construction of Lagrangian L and dissipation Φ functions. In principle, the Lagrangian function includes the conservative characteristics of the system, while the dissipation function incorporates the non-conservative aspects. Both are functions of the generalized coordinates q_k of the system and their first-order time derivatives for $k=1, \ldots, n$. The action integral is introduced and by applying Hamilton's action principle (Hamilton, 1834) one arrives at the Euler-Lagrange equations, which are the governing equations of the system.

Partitioning the degrees of freedom (DOF) of the structure into those that have associated mass or damping, those that do not have mass or damping, and those with prescribed displacement or velocity, the governing equations of the structure are (Apostolakis *et al*., 2011):

$$\mathbf{M\dot{v}} + \mathbf{Cv} + \mathbf{B}_1\mathbf{F} = \mathbf{P} \tag{1a}$$

$$\mathbf{A\dot{F}} + \partial_{\mathbf{F}}\Phi\left(\mathbf{F},\boldsymbol{\zeta}\right) - \mathbf{B}_1^{\mathrm{T}}\mathbf{v} - \mathbf{B}_2^{\mathrm{T}}\mathbf{v}^{\mathbf{o}} - \mathbf{B}_3^{\mathrm{T}}\mathbf{v}^{\mathbf{p}} = \mathbf{P} \tag{1b}$$

$$\mathbf{B}_2\mathbf{F} = \boldsymbol{\Pi} \tag{1c}$$

$$\mathbf{G}\dot{\boldsymbol{\zeta}} + \partial_{\zeta}\Phi\left(\mathbf{F},\boldsymbol{\zeta}\right) = \mathbf{0} \tag{1d}$$

where **M** is the mass matrix, **C** is the damping matrix, **B** is the equilibrium matrix, **A** is the block diagonal matrix of element flexibilities, **G** is the block diagonal matrix of inverse hardening moduli, **F** is the vector of internal forces in the structure, **v** is the vector of velocities at DOF with associated mass or damping, $\mathbf{v}^{\mathbf{o}}$ is the vector of velocities at DOF with neither mass nor damping (quasi-static), $\mathbf{v}^{\mathbf{p}}$ is the vector of velocities at DOF with prescribed displacement/velocity, $\boldsymbol{\zeta}$ is the vector of internal variables (for plasticity, etc.), **P** is the vector of external forces on DOF with mass or damping, $\boldsymbol{\Pi}$ is the vector of external forces at quasi-static DOF. When geometric nonlinearities is considered, the equilibrium matrix **B** is a function of displacement, and is partitioned as $\mathbf{B}=[\mathbf{B}_1^{\mathrm{T}}, \mathbf{B}_2^{\mathrm{T}}, \mathbf{B}_3^{\mathrm{T}}]^{\mathrm{T}}$ corresponding to DOF with mass or damping, quasi-static DOF, and DOF with prescribed displacement or velocity, respectively. The governing equations include the linear momentum equation, the deformation compatibility in the elements equation, the equilibrium equation at quasi-static DOF, and the evolution of constitutive internal variables equation, respectively.

The governing equations obtained by the Lagrangian formalism are solved numerically with a discrete variational integrator based on Cadzow's discrete calculus of variations (Cadzow, 1970). Starting by constructing a discrete Lagrangian L_d, which is an approximation of the continuous Lagrangian L, the discrete action sum S_d that corresponds to L_d is constructed, where

$$S_d = \sum_{k=1}^{N} L_d\left(q_{k-1}, q_k\right) \tag{2}$$

while N is the total number of time–steps and q_k represents the discrete value of a state variable at step k.

Following Cadzow's discrete variational calculus, the solution of the discrete system governed by the Lagrangian L_d is the one that produces the extreme discrete action sum S_d. The action integral is discretized using the midpoint rule with a time-step h. It can be shown that if either the internal force **F** or velocity **v** state variables are eliminated from the above set of discrete equations, then the remaining set of equations can be defined as a minimization problem. The minimization problem, in terms of internal force vector **F** as state variable, can be restated as:

$$\left(\mathbf{F}_{n+1}, \boldsymbol{\zeta}_{n+1}\right) = \arg\min \frac{1}{2}\mathbf{F}^{\mathrm{T}}\left(\mathbf{A} + \frac{h^2}{4}\mathbf{B}_1^{\mathrm{T}}\tilde{\mathbf{M}}^{-1}\mathbf{B}_1\right)\mathbf{F} + \frac{1}{2}\boldsymbol{\zeta}^{\mathrm{T}}\mathbf{G}\boldsymbol{\zeta} - \boldsymbol{\beta}^{\mathrm{T}}\mathbf{F} - \boldsymbol{\gamma}^{\mathrm{T}}\boldsymbol{\zeta}$$

$$\text{Subject to } \mathbf{B}_2\mathbf{F} = \boldsymbol{\Pi}_{n+1} \tag{3}$$

$$\text{and } \frac{h}{2}\varphi\left(\mathbf{F}\right) \le 0$$

where the yield function of the structure *φ(.)* appears as a constraint. The minimization problem (3) is solved as a sequence of linear equality-constraint problems, where the constraints are represented by an augmented Lagrangian approach. For a detailed presentation of the minimization approach, the reader is referred to Sivaselvan *et al*. (2006, 2009).

The MLF approach has been extended to fully coupled thermoelasticity and poroelasticity (Apostolakis, 2010) and a Mixed Lagrangian Formulation for linear thermoelastic response of structures has been developed (Apostolakis and Dargush, 2012). The above can be used to study the behavior of structures under thermal loads (fire) and for soil-structure interaction analysis of structures. This will be the matter of interest in future work.

2.2. Optimization algorithm

Genetic algorithms (GAs) employ a population of solutions as the initial seed and then, with the use of stochastic selection, crossover and mutation operators, evolve to produce improving solutions. GAs owe their power mainly to selection and crossover operators, while the mutation operator has only secondary significance. The limited role of mutation is evident from the low mutation rates used in most GAs. On the other hand, cellular automata (CA) use localized structures and operators to solve problems in an evolutionary way. In the most interesting cases, CA display a significant ability toward self-organization that derives from the local structure. A new CA-GA framework was developed in Barmpoutis and Dargush (2007) to take advantage of these self-organizing characteristics of CAs, while retaining the attractive features of the GA evolutionary process. Within this algorithm, which is applied here for the first time in seismic design, every individual of the population is assigned to a cell and the number of CA lattice cells is equal to the number of individuals in the population. Then, within this framework, an iteration of the CA corresponds to a generation of the GA. However, the CA-GA approach abandons global statistics that control the evolution of the population in a standard GA. Instead, local rules involving nearest neighbors direct the evolution on the lattice. Further details are provided in Barmpoutis and Dargush (2007).

2.3. Evaluation criteria and fitness function

A fitness function f is defined, based upon inter-story drifts and absolute accelerations, to direct the development of robust design solutions under seismic loading. Let $\Delta_i^{(k)}(t)$ and $a_i^{(k)}(t)$ represent the drift and acceleration, respectively, of the i^{th} story at time t for the k^{th} earthquake. Then, the fitness of the structure for earthquake k can be written

$$f_k = 2\left(\frac{\max|\Delta_i^{(k)}(t)|}{\Delta_{\text{allow}}} + \frac{\max|a_i^{(k)}(t)|}{a_{\text{allow}}} \right)^{-1} \tag{4}$$

where Δ_{allow} and a_{allow} represent the allowable levels for drift and acceleration, respectively. Notice that if drifts and accelerations are both at their allowable limits, the fitness function for the earthquake equals unity. Finally, the overall fitness for the structure is defined as the minimum value of f_k, taken over all of the earthquakes. Thus,

$$f = \max\left\{ f_1, f_2, \ldots, f_n \right\} \tag{5}$$

Equations (4) and (5) apply for unconstrained brace topological optimization problems, which permit the selection of the maximum number and sizes of braces throughout the structure. On the other hand, when a constraint is introduced on the total number of brace element sets, a penalty formulation is used to reduce f dramatically if this limiting value is exceeded. For example, let n_b and $n_{b,\text{limit}}$ represent the number of brace sets in a given structure and the limiting number, respectively. Then, for the constrained problem,

$$f = \frac{\max\left\{ f_1, f_2, \ldots, f_n \right\}}{1 + \left\langle n_b - n_{b,\text{limit}} \right\rangle} \tag{6}$$

where $\langle . \rangle$ denotes the Macauley bracket function.

3. STRUCTURES

The three-dimensional structures considered in the present study are three-, eight- and fifteen-story steel frame buildings, along with an irregular eight-story steel frame building. The floor plan and elevation views of the buildings are presented in Fig. 1. The location of the moment-resisting frames is in the perimeter of the buildings and it is shown with bold lines in the floor plans. For the eight-story irregular building, the floor plan is as shown up to the sixth floor and the shaded area indicates the floor plan for the two upper floors. The column bases in all building are considered as fixed. All the columns in the perimeter moment-resisting frames bend about the strong axis. The strong axis of the gravity columns is assumed to be oriented in the NS direction.

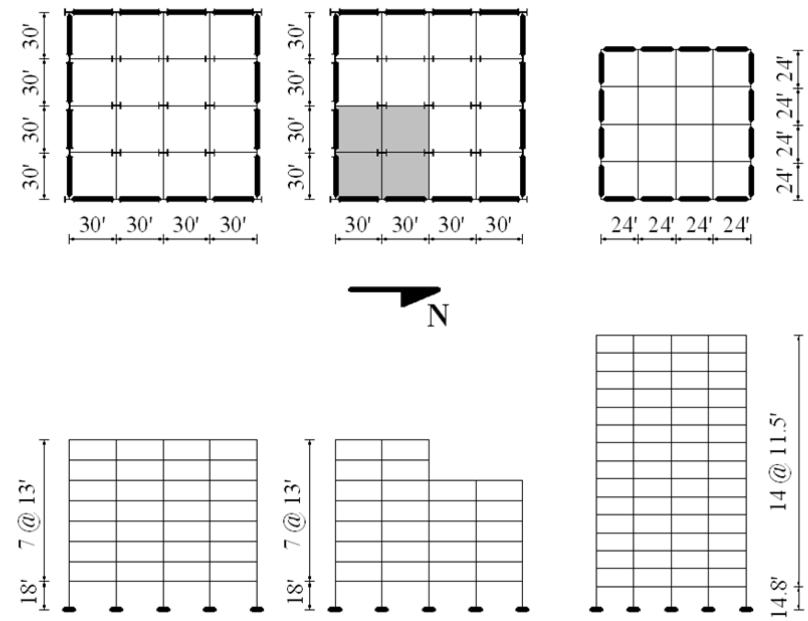

Figure 1. Floor plans and elevation views for the regular eight-, irregular eight- and fifteen-story building

The sections used for the NS direction frames are summarized in Table 1. In all the cases, the design of the moment-resisting frames in EW direction was assumed identical to the ones in the NS direction. The design yield strength of the beams is 248 MPa (36 ksi) and for the columns is 344 MPa (50 ksi). The seismic mass for the structures is summarized in Table 1.

Table 1. Column Sections, Beam Sections and Seismic Mass for the Three-Dimensional Buildings

8-story Regular Building						
Story	NS Moment-Resisting Frames			NS Gravity Frames		Seismic Mass (metric tonne)
	Column		Beam	Column	Beam	
	Exterior	Interior				
1	W14x370	W14x500	W36x160	W14x193	W21x44	644.839
2	W14x370	W14x500	W36x160	W14x193	W18x35	633.818
3	W14x370	W14x500	W36x160	W14x193	W18x35	633.818
4	W14x370	W14x455	W36x135	W14x145	W18x35	633.818
5	W14x370	W14x455	W36x135	W14x145	W18x35	633.818
6	W14x283	W14x370	W36x135	W14x109	W18x35	633.818
7	W14x283	W14x370	W36x135	W14x109	W18x35	633.818
8	W14x257	W14x283	W30x99	W14x82	W18x35	682.760

Note: 1. The eight-story irregular building has same section properties and seismic mass as the eight story building. For the last two floors assume proportional seismic mass to the floor plan area.
2. For information on the fifteen-story building contact the authors.

4. DESIGN APPLICATIONS

The design applications presented in this paper include the regular and irregular eight-story structures. The fitness function defined in Section 2.3 above is used with parameters Δ_{allow} = 1.5%, α_{allow} = 1.0g.

The first design parameter is a target maximum inter-story drift, taken as the life safety (S-3) 1.5% drift limit for braced steel frames from Table C1-3 FEMA-356 (2000). The second design parameter is a target maximum story acceleration of 1.0 g, for non-structural components. In case studies where we assume that X-type brace configurations are available but with a penalty, we assume $n_{b,\mathrm{limit}} = 5$. Below the optimization parameters and the seismic environment assumed in the optimization are presented.

4.1. Optimization parameters

In this section, the parameters that will be optimized are established. For the retrofitted three-dimensional structures, the optimization parameters are the damper configuration D_{conf}, the damper area A_d, and the damper yielding force $F_{y,d}$. For the design applications presented in this paper a post-yield ratio of $\alpha=10^{-3}$ is assumed. A multi-scale approach is assumed for the damper configuration by assuming brace pattern configurations that span 2-by-2 bays. The possible configuration patterns assumed are eight and are shown in Table 2. The number of values that the damper area A_d, and the damper yielding force $F_{y,d}$ parameters each could take is four, which are summarized in Table 2.

Table 2. Optimization parameter values and configuration for hysteretic dampers

Damper parameter values/configuration				
Damper Configuration, D_{conf} (2x2 bays)	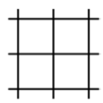	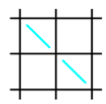	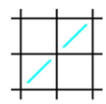	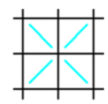
	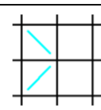	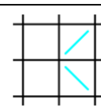	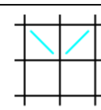	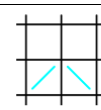
Area, A_d	1.290E-03 (2)	2.581E-03 (4)	5.161E-03 (8)	1.0323E-02(16)
Yield force, $F_{y,d}$	88.964 (20)	177.929 (40)	355.858 (80)	711.716 (160)
Note: Units are [m – kN]	(in parenthesis are the values in [kips – in.])			

4.2. Seismic environment

The earthquake environment of the design application was selected from the MCEER synthetic ground motions representative of the west coast of the United States. The MCEER west coast ground motions consist of 100 synthetic near fault ground motions. The 100 ground motions correspond to four different return periods of 250, 500, 1000 and 2500 years. These time histories are the samples of a Gaussian process with a spectrum that is based on a physical model, the Specific Barrier Model. The Specific Barrier Model was proposed and developed by Papageorgiou and Aki (1983a, b; 1985) for the quantitative description of heterogeneous rupture. It provides a physical description of the faulting processes responsible for the generation of high-frequency waves. The specific barrier model has been calibrated by Halldorsson and Papageorgiou (2005) to a strong motion database. The 5% probability of exceedance in 50 years earthquakes (25 EQs) was used as the pool for the seismic environment of the design applications. The earthquakes that were selected were number 10 (EQ10), 21 (EQ21), 22 (EQ22), and 25 (EQ25). The same four earthquakes are used for all three structures included in the design application study of this paper. For more information about the earthquakes, the reader is referred to Apostolakis (2006) and Wanitkorkul and Filiatrault (2005).

Under realistic conditions the direction of the earthquake is rarely perfectly aligned with one of the orthogonal directions of a three-dimensional structure in plan-view. In order to accommodate for the above, the direction of each Earthquake in plan-view with regard to the N-S direction (see Fig. 1) was randomly generated. For earthquakes EQ10, EQ21, EQ22 and EQ25, the resulting direction angles were established as 27°, 63°, 78°, 11°, respectively.

5. RESULTS

Three case studies are performed for the regular eight-story structure. In the first case we assume that all brace configurations from Table 2 are available during the optimization, in the second case we assume that there are not X-type brace configurations available, while in the last case we assume that X-type brace configurations are available but with a penalty as defined in Section 2.3.

In Fig. 2, the optimal design solutions for each of the three case studies are shown for the regular eight-story structure. The topological distributions of the braces throughout the height of the structure correspond to patterns that are not seen in common practice. It is observed that X-type brace configurations are favored in the bottom half of the structure with bigger sized dampers and high yield force levels. This is explained by the increased height of the first story comparing to the other stories, and by the fact that the base structure had maximum drift values appearing at the bottom half of the structure. On the top third of the structure, dampers with lower yield force levels are selected. This can be explained by the fact that the base structure had the peak acceleration values at the top stories. As a result, the optimization evolved to a solution that reduces the drifts while controlling and even reducing accelerations.

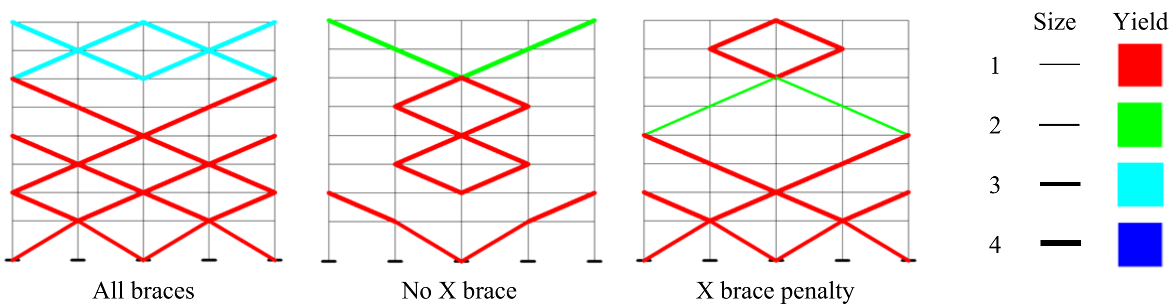

Figure 2. Topology optimization for regular eight-story structure

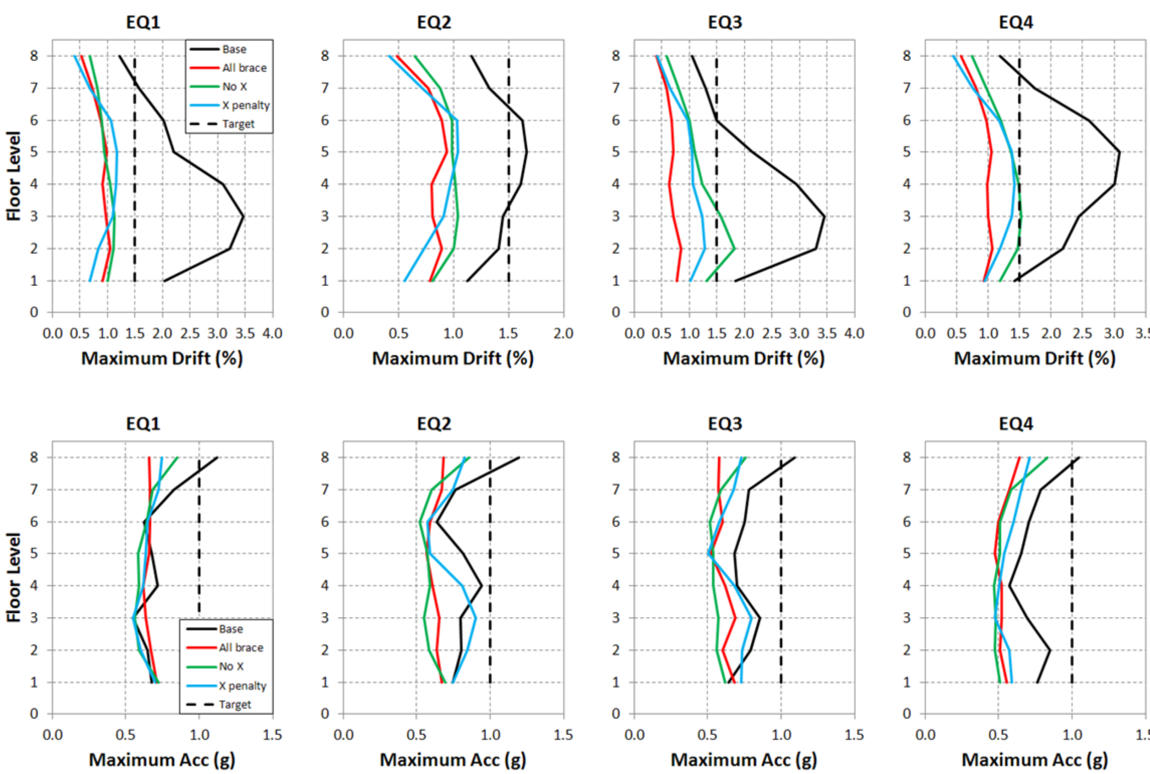

Figure 3. Base and optimal retrofitted designs response comparison for the regular eight-story structure

The distribution of maximum inter-story drift and maximum acceleration throughout the height of the regular eight-story structure for all earthquakes are presented in Fig. 3. It is observed that all the retrofitted design solutions, except for the case with no X-type braces and for EQ3, have drift and acceleration values well below the target drift of 1.5% and acceleration of 1g, respectively. Thus, the retrofitted optimal designs satisfy the 1.5% life-safety drift limit while the base structure was close to collapse, per FEMA-356 (2000). The optimization framework proposed in this paper produced optimal designs with reduced drifts while reducing accelerations at the same time. Moreover, the optimal designs evolved towards a uniform distribution of drifts and accelerations. As a result, the ductility demand is uniformly distributed throughout the height of the retrofitted structure. Evidently this provides with an optimal utilization of the hysteretic dampers.

For the irregular eight-story structure two case studies are performed. In the first case we assume that there are not X-type brace configurations available (see Table 2), while in the last case we assume that X-type brace configurations are available but with a penalty. In Fig. 4, the optimal design solutions for each of the two case studies are shown. Again, the topological distributions of the braces throughout the height of the structure correspond to patterns that are not seen in common practice. Similar observations can be made for the bottom half of the structure as for the regular eight-story structure optimal designs. Interestingly, for the irregular eight-story structure it is observed that just below the vertical irregularity of the structure the optimal dampers have low yield force levels. While for the top two floors high yield force values are selected. Thus, the optimization evolved into solutions that reduce the drift and acceleration by retrofitting with dampers in a way that more stress is not added to the structure due to the discontinuity of the floors at the six story level.

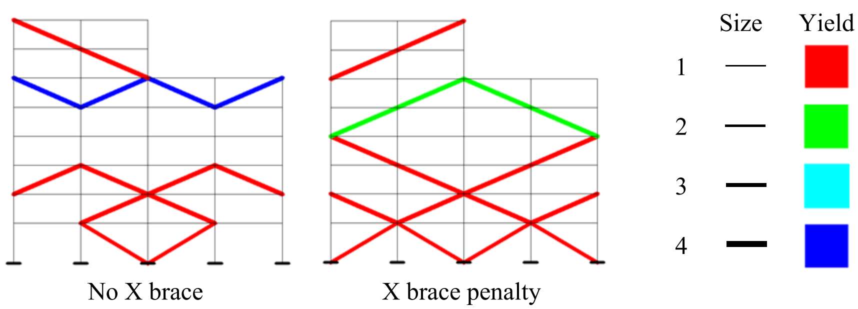

Figure 4. Topology optimization for irregular eight-story structure

The distribution of maximum inter-story drift and maximum acceleration throughout the height of the irregular eight-story structure for all earthquakes are presented in Fig. 5. Again, it is observed that for all the design solutions, except for the case with no X-type braces and for EQ4, the retrofitted designs have drift and acceleration values well below the target drift of 1.5% and acceleration of 1g, respectively. Thus, the retrofitted optimal designs satisfy the 1.5% life-safety drift limit while the base structure was close to collapse, per FEMA-356 (2000). Concluding, the optimization framework proposed in this paper produced optimal designs where the drifts were reduced while reducing accelerations at the same time. Again, the optimal designs evolved towards a uniform distribution of drifts and accelerations and an optimal utilization of the dampers was achieved.

6. SUMMARY

Current seismic codes incorporate well-established simplified approaches to protect and mitigate the response of structures under extreme events using hysteretic passive devices. Nevertheless, a systematic and well-establish methodology for the topological distribution and properties of these devices in three-dimensional structures does not exist. In this paper, we develop a computational framework to evolve optimal brace configurations for complicated three-dimensional regular and irregular structures within a given seismic environment consisting of four synthetic ground motions (5% exceedance in 50 years). Non-linear transient dynamic analyses, based upon a Mixed Lagrangian formulation, are used to evaluate the structures, while the optimization is accomplished with a compact Cellular Automata-based Genetic Algorithm.

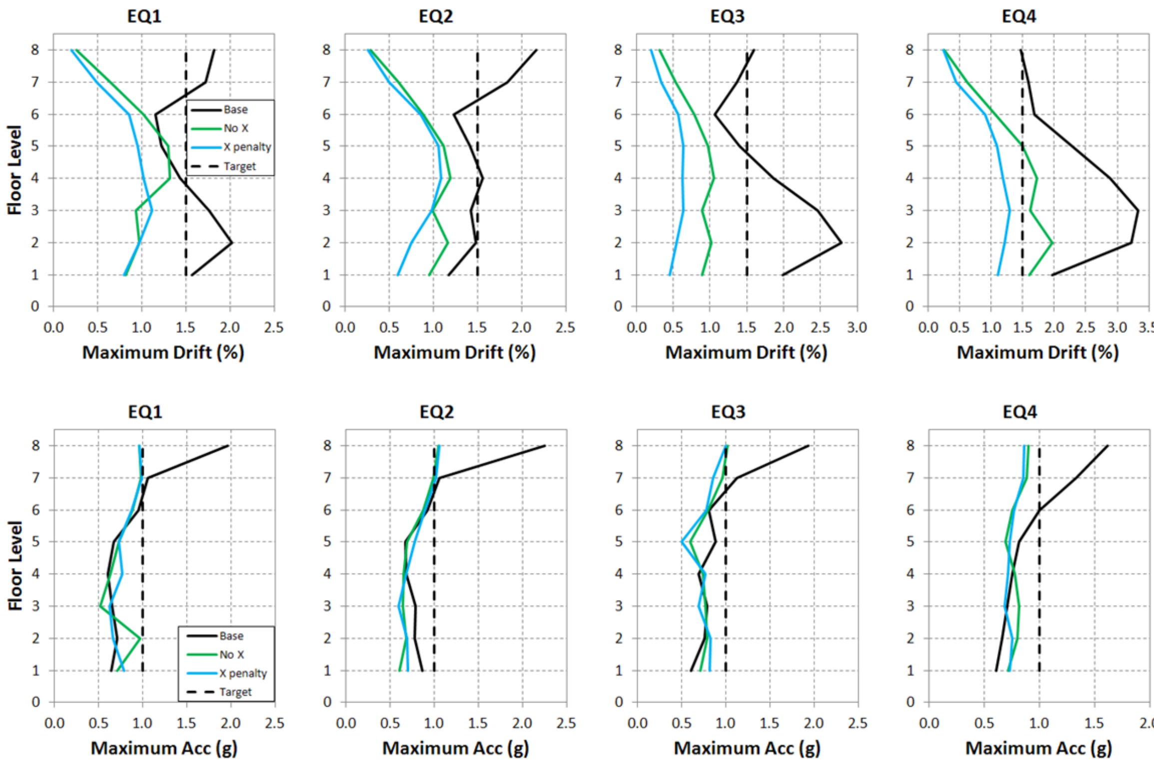

Figure 5. Base and optimal retrofitted designs response comparison for the irregular eight-story structure

The computational framework proposed herein is applied to the retrofit of regular and irregular eight-story three-dimensional structures. From the evolutionary process, the optimal placement, strength and size of the dampers throughout the height of the structures are obtained. The topological distributions of the braces throughout the height of the structure correspond to patterns that are not seen in common practice. For all the design applications, the optimization resulted in retrofitted structures that satisfied the predefined design target drift limit of 1.5% and design target acceleration limit of 1.0g. Therefore, the retrofitted optimal designs satisfy the 1.5% life-safety drift limit while the original base structures were close to collapse, per FEMA-356 (2000). It is noteworthy to mention that the optimization framework proposed in this paper produced optimal designs with reduced drifts while reducing accelerations at the same time.

From the design applications of this paper, it is recommended that, in order to satisfy the life-safety drift limits required by modern code and for optimal utilization of the braces, the retrofitted schemes should be based on ductility demand throughout the height of the yielded structure under the earthquake environment of interest, rather than on the elastic modes as in common practice. During the evolution of the proposed optimization framework, the optimal designs evolved towards a uniform distribution of drifts and accelerations. The ductility demand is uniformly distributed throughout the height of the retrofitted structure, consistent with results in Levy and Lavan (2006), Lavan and Dargush (2009) and Apostolakis and Dargush (2010). Evidently this provides with an optimal utilization of the hysteretic dampers. The proposed computational framework appears to be an attractive alternative for the seismic design and retrofit of realistic three-dimensional structures with hysteretic passive dampers. The computational and engineering effort is modest and well within the range of typical seismic design firms.

REFERENCES

Apostolakis G. (2010). A Lagrangian Approach for Thermomechanics towards Damage and Deterioration of Structures, Ph.D. dissertation, University at Buffalo, State University of New York, Buffalo, NY.

Apostolakis G. (2006). Evolutionary Aseismic Design of Self-Centering Post-Tensioned Energy Dissipating Steel Frames. MS Thesis, University at Buffalo, State University of New York, Buffalo, NY.

Apostolakis G. and Dargush G. F. (2012). Mixed Lagrangian Formulation for Linear Thermoelastic Response of Structures, *J. Engrg. Mechanics* (ASCE), **138:5**, 508-518.

Apostolakis G., Reinhorn A. M., Dargush G. F., Lavan O., and Sivaselvan M. (2011). Analysis of Collapse of Irregular Tall Structures using Mixed Lagrangian Formulation, *Sixth European Workshop on Irregular and Complex Structures 6EWICS*, 12-13 September, Haifa, Israel.

Apostolakis G., Dargush G.F. (2010). Optimal Seismic Design of Moment Resisting Steel Frames with Hysteretic Passive Devices, *Earthquake Engrg. Struct. Dyn.*, **39:4**, 355-376.

Barmpoutis V., Dargush G.F. (2007). A Compact Self-Organizing Cellular Automata-Based Genetic Algorithm, arXiv:0711.2478v1 [cs.NE].

Cadzow J.A. (1970). Discrete Calculus of Variations, *International Journal of Control*, **11:3**, 393-407.

Dargush G.F., Sant R.S. (2005). Evolutionary Aseismic Design and Retrofit with Passive Energy Dissipation, *Earthquake Engrg. Struct. Dyn.*, **34:13**, 1601-1626.

FEMA-356 (2000). Prestandard and Commentary for the Seismic Rehabilitation of Buildings. Report No. FEMA 356, Federal Emergency Management Agency, Washington, DC.

FEMA-273 (1997). NEHRP Guidelines for the Seismic Rehabilitation of Buildings. Bldg. Seis. Safety Council.

FEMA-274 (1997). Commentary to NEHRP Guidelines for the Seismic Rehabilitation of Buildings. Bldg. Seis. Safety Council.

Gluck N., Reinhorn A.M., Gluck J., Levy R. (1996). Design of Supplemental Dampers for Control of Structures, *J. Struct. Engrg.* (ASCE), **122:12**, 1394 –1399.

Halldorsson B., Papageorgiou A.S. (2005). Calibration of the Specific Barrier Model to Earthquakes of Different Tectonic Regions, *Bulletin of the Seismological Society of America*, **95:4**, 1276-1300.

Hamilton W.R. (1834). On a General Method in Dynamics, *Philosophical Transactions of the Royal Society of London*, *The Royal Society*, **124**, 247-308.

Holland J.H. (1992). Adaptation in Natural and Artificial Systems. Second edition, MIT Press.

Lavan O., Levy R. (2005). Optimal Design of Supplemental Viscous Dampers for Irregular Shear-Frames in the Presence of Yielding, *Earthquake Engrg. Struct. Dyn.*, **34:8**, 889-907.

Lavan O., Levy R. (2006). Optimal Peripheral Drift Control of 3D Irregular Framed Structures Using Supplemental Viscous Dampers, *J. Earthquake Engrg.*, **10:6**, 903-923.

Lavan O., Dargush G.F. (2009). Multi-Objective Evolutionary Seismic Design with Passive Energy Dissipation Systems, *J. Earthquake Engrg.*, **13:6**, 758-790.

Levy R., Lavan O. (2006). Fully Stressed Design of Passive Controllers in Framed Structures for Seismic Loadings, *Struct. Multidisciplinary Opt.*, **32:6**, 485-498.

Moreschi L.M., Singh M.P. (2003). Design of Yielding Metallic and Friction Dampers for Optimal Seismic Performance, *Earthquake Engrg. Struct. Dyn.*, **32:8**, 1291-1311.

Papageorgiou A.S., Aki K. (1985). Scaling Law of Far-Field Spectra Based on Observed Parameters of the Specific Barrier Model, *Pure and Applied Geophysics*, **123:3**, 353-374.

Papageorgiou A.S., Aki K. (1983a). A Specific Barrier Model for the Quantitative Description of Inhomogeneous Faulting and the Prediction of Strong Ground Motion. 1. Description of the Model, *Bulletin of the Seismological Society of America*, **73:3**, 693-722.

Papageorgiou A.S., Aki K. (1983b). A Specific Barrier Model for the Quantitative Description of Inhomogeneous Faulting and the Prediction of Strong Ground Motion. 2. Applications of the Model, *Bulletin of the Seismological Society of America*, **73:4**, 953-978.

Prakash V. (1993). *Drain-2DX—Inelastic Dynamic 2d Analysis Program*. University of California Berkeley, Berkeley, CA.

Singh M.P., Moreschi L.M. (2001). Optimum Seismic Response Control with Dampers, *Earthquake Engrg. Struct. Dyn.*, **30:4**, 553–572.

Singh M.P., Moreschi L.M. (2002). Optimal Placement of Dampers for Passive Response Control, *Earthquake Engrg. Struct. Dyn.*, **31:4**, 955–976.

Sivaselvan M.V., Lavan O., Dargush G.F., Kurino H., Hyodo Y., Fukuda R., Sato K., Apostolakis G., Reinhorn A.M. (2009). Numerical Collapse Simulation of Large-Scale Structural Systems Using an Optimization-Based Algorithm, *Earthquake Engrg. Struct. Dyn.*, **38:5**, 655-677.

Sivaselvan M.V., Reinhorn A.M. (2006). Lagrangian Approach to Structural Collapse Simulation, *J. Engrg. Mechanics* (ASCE), **132:8**, 795-805.

Soong T.T., Dargush G.F. (1997). *Passive Energy Dissipation Systems in Structural Engineering*, Wiley.

Takewaki I. (1997). Optimal Damper Placement for Minimum Transfer Functions, *Earthquake Engrg. Struct. Dyn.*, **26:11**, 1113-1124.

Wanitkorkul A., Filiatrault A. (2005). Simulation of Strong Ground Motions for Seismic Fragility Evaluation of Nonstructural Components in Hospitals. MCEER-05-0005, University at Buffalo, Buffalo, NY.

Zhang R.H., Soong T.T. (1992). Seismic Design of Viscoelastic Dampers for Structural Applications, *J. Struct. Engrg.* (ASCE), **118:5**, 1375 –1392.